HHS Public Access

Author manuscript

J Neuroimaging. Author manuscript; available in PMC 2023 February 10.

Published in final edited form as:

J Neuroimaging. 2010 January ; 20(1): 87–92. doi:10.1111/j.1552-6569.2008.00331.x.

Double Inversion Recovery MRI with Fat Suppression at 7 Tesla: Initial Experience

Guillaume Madelin, PhD,

Niels Oesingmann, PhD,

Matilde Inglese, MD, PhD

Department of Radiology, New York University, New York, NY (GM, MI); Siemens Medical Solutions USA, Inc. (NO)

Abstract

BACKGROUND AND PURPOSE—Double Inversion Recovery Magnetic Resonance Imaging (DIR) consists of two adiabatic non-selective inversion pulses applied before a Turbo Spin Echo (TSE) sequence, in order to suppress the signal from two tissues with different longitudinal relaxation times T_1 simultaneously. In the brain, DIR is used to selectively image the gray matter (GM) by nulling the signal from white matter (WM) and cerebrospinal fluid (CSF). The main limitation of the technique remains the intrinsic low SNR due to the specific preparation of the longitudinal magnetization. The recent availability of high field magnets operating at 7 T for human imaging offers the advantage of higher SNR. This study shows the feasibility of brain Double Inversion Recovery Magnetic Resonance Imaging (DIR-MRI) at 7 T in vivo in healthy volunteers.

METHODS—The MRI experiments were performed on phantoms at 7 T and on four healthy volunteers at 7 and 3 T. For fat suppression, a chemical shift selective Fat Inversion Recovery (csFatIR) technique was used and compared to the standard fat saturation (FatSat).

RESULTS—The csFatIR method resulted to be significantly more efficient than the Fatsat at 7 T and slightly more efficient at 3 T, enabling a clear delineation of GM.

CONCLUSIONS—DIR is feasible at 7 T despite the problems associated with B_1 in-homogeneity.

Keywords

Double inversion recovery; fat suppression; high field MRI

Introduction

Double Inversion Recovery Magnetic Resonance Imaging (DIR-MRI) consists of two inversion pulses preceding a conventional spin-echo sequence, which allow simultaneous suppressing of the signals from two tissues with different T_1 relaxation times.[1,2] In the

Correspondence: Address correspondence to Matilde Inglese, MD, PhD, New York University Medical Center, Center for Biomedical Imaging, 650 First Avenue, 6th Floor, New York, NY 10016. matilde.inglese@med.nyu.edu.

brain, DIR can be used to selectively image the gray matter (GM), while the signal from white matter (WM) and cerebrospinal fluid (CSF)[2–6] is minimized. Despite the inherent limitation due to the thin and folded structure of the cortex, the visualization of GM is important in the evaluation of normal subjects and in patients with multiple sclerosis (MS), cerebral ischemia, epilepsy, degenerative diseases, and tumors.[7–9] Not only can DIR be used to assess global and regional cortical thickness and lesions, but it also provides a method for improving GM segmentation and limits the partial volume effect.[4]

Previous studies successfully implemented DIR as 2-dimensional and 3-dimensional sequence at 1.5 and 3 T.[3,5] Although 3-dimensional acquisition improves signal-to-noise ratio (SNR) per unit time and resolution, the main limitation of the technique remains the intrinsic low SNR due to the specific preparation of the longitudinal magnetization. The recent availability of high field magnets operating at 7 T for human imaging offers the advantage of higher SNR[10] and higher spatial resolution, while maintaining acquisition times that are compatible with patients' compliance. However, ultra-high field imaging is accompanied by several drawbacks such as an increase of susceptibility artifacts, higher B_0 and B_1 inhomogeneities, and larger power deposition.[10–12] This requires a careful implementation and optimization of pulse parameters, imaging protocols, and fat saturation techniques. Specifically, we noticed that the standard fat signal suppression method was insufficient in brain DIR images acquired at 7 T, leading to artifacts that hamper a clear delineation of GM.

In this communication, we describe theoretically and experimentally a multiple inversion method with the implementation of a chemical shift selective fat inversion recovery (csFatIR) pulse to the 2-dimensional and single-slab 3-dimensional DIR preparation scheme to simultaneously suppress the large signal contributions from brain WM, CSF, and surrounding fat tissue. The same method is applied at 7 and at 3 T. The method improves overall brain tissue contrast and visualization of GM at 7 T compared to 3 T.

Theory

The DIR sequence was implemented by adding two non-selective adiabatic inversion pulses to a standard Turbo Spin Echo (TSE) sequence. The first inversion time TI_1 is defined as the time between the first and the second inversion pulse. The second inversion time TI_2 is the time between the second inversion pulse and the 90° excitation of the imaging sequence. A third non-selective adiabatic inversion pulse is added to this preparation scheme for chemical shift selective fat inversion recovery applied at the fat frequency (csFatIR). Since the fat chemical shift is around 3.5 ppm, the fat frequency shift is around −430 Hz at 3 T and −1 kHz at 7 T. The inversion time TI_{fat} is the time between the fat inversion pulse and the 90° excitation pulse. The sequence pulse chronogram is described in Figure 1.

According to the Bloch equations,[13] the available magnetization M_A prior to the 90° pulse of the DIR TSE is

$$M_A = M_0\left[1 - 2(1 - E_1)E_2 - E_{TR}E_{TE}^{-1}\right] \quad (1)$$

with the parameters $E_1 = \exp(-\mathrm{TI}_1/T_1)$, $E_2 = \exp(-\mathrm{TI}_2/T_1)$, $E_{\mathrm{TR}} = \exp(-\mathrm{TR}/T_1)$, $E_{\mathrm{TE}} = \exp(-N\tau/T_1) = \exp(-2\,TE_{\mathrm{eff}}/T_1)$, the original magnetization at equilibrium M_0, the repetition time TR, the effective echo time $\mathrm{TE}_{\mathrm{eff}}$, the number of echos (turbo factor) N, the echo spacing τ, and the longitunal relaxation time T_1. This equation is valid when $\tau << T_1$, which is generally the case in our experiments as τ is in the range of a few milliseconds and T_1 in the range of several hundred miliseconds. We use the graphical method described by Redpath and Smith[2] to find the TI_1 and TI_2 required to null the signal from two tissues with different T_1 and for different TR. The method consists of plotting TI_2 as a function of TI_1, with the assumption of $M_{\mathrm{A}} = 0$ for the two different T_1, and TR as constant parameter:

$$\mathrm{TI}_2 = T_1 \ln\left[\frac{2(1 - E_1)}{1 - E_{\mathrm{TR}}E_{\mathrm{TE}}^{-1}}\right]. \quad (2)$$

As a consequence, the two curves intercept at the point giving TI_1 and TI_2. This calculation is repeated for different TRs, in order to obtain TI_1 and TI_2 for simultaneous suppression of two tissues as a function of TR.

The following T_1 values for the tissues were used: at 3 T, $T_1^{\mathrm{WM}} = 830$ ms, $T_1^{\mathrm{GM}} = 1300$ ms, $T_1^{\mathrm{CSF}} = 4300$ ms, and at 7 T, $T_1^{\mathrm{WM}} = 1220$ ms, $T_1^{\mathrm{GM}} = 1950$ ms, $T_1^{\mathrm{CSF}} = 4300$ ms. These T_1 values are average values taken from references[4,14–16] and experiments. The fitting parameters A, B, and C of the fitting function $\mathrm{TI(TR)} = A + B \cdot e^{C \cdot \mathrm{TR}}$ are given in Table 1, and the curves are shown in Figure 2. Although the fitting curves show that TRs longer than 10 s are preferable to achieve an optimal differentiation between WM + CSF and GM + CSF suppression, we used a TR of 5 s which allows a sufficient differentiation of the different tissues in a reasonable scan time for the patients.

Inversion Pulses

All adiabatic (hyperbolic secant) inversion pulses used in the present study have a bandwidth-time-product of $T_{\mathrm{p}}\Delta\nu = 15.26$, with T_{p} the pulse duration and $\Delta\nu$ the bandwidth. These parameters were optimized empirically on phantoms simulating different tissues and then applied on brain in vivo: At 3 T, DIR $T_{\mathrm{p}} = 12$ ms, $\Delta\nu = 1.27$ kHz; csFatIR $T_{\mathrm{p}} = 30$ ms, $\Delta\nu = 508$ Hz. At 7 T, DIR $T_{\mathrm{p}} = 10.24$ ms, $\Delta\nu = 1.5$ kHz; csFatIR $T_{\mathrm{p}} = 14$ ms, $\Delta\nu = 1.1$ kHz. Large bandwidths for DIR were first adjusted to obtain a maximum suppression of the chosen tissues. The bandwidth of csFatIR was adjusted subsequently to optimize fat suppression while affecting the water signal as less as possible.

Material and Methods

This study was performed on a 7 T whole body magnet (Siemens Medical Solutions, Erlangen, Germany) using a 24-channel head coil (Nova Medical Inc., Wilmington, MA) and on a 3 T magnet (Tim Trio, Siemens Medical Solutions) using the Siemens system's 12-channel head coil.

Phantom Experiments

The phantom experiments were performed at 7 T to show the efficiency of the csFatIR pulse compared to the standard fat saturation (FatSat). Three different phantoms were imaged concurrently: one bottle of vegetable oil (simulating fat), T_1 = 330 ms, one bottle of gel Agar 4% + NaCl 15 mM, T_1 = 2470 ms, and one bottle of the following solution: $6H_2O$ + $CuSO_4$ 1.78 g/L + NaCl 1.61 g/L, T_1 = 190 ms. The acquisition parameters were 2-dimensional TSE, TE = 41 ms, TR = 5000 ms, FOV = 220 × 155 mm, bandwidth = 500 Hz/pixel, matrix = 256 × 180, resolution = .86 mm × .86 mm × 5 mm, number of echoes = 15, Time of acquisition = 1 min. For the suppression of the gel and solution signals by DIR, for this TR, the inversion times were calculated using the Redpath method previously described: TI_1 = 1500 ms and TI_2 = 130 ms. For csFatIR, TI_{fat} = 230 ms.

Human Experiments

The theoretical inversion times for DIR were evaluated according to the Redpath method and used as initial values for parameter optimization by scanning a healthy volunteer. This scan matched the MRI parameters of the subsequent DIR scans. Increments in steps of 10-20 ms of TI_1 and TI_2 were used to find the optimal WM and CSF nulling TIs, for TR = 5000 ms : TI_1 = 2100 ms, TI_2 = 470 ms, TI_{Fat} = 90 ms at 3 T and TI_1 = 2180 ms, TI_2 = 550 ms, TI_{Fat} = 310 ms at 7 T.

Once the TIs needed to selectively image WM and GM had been determined, four volunteers (two women and two men; mean age: 26; range: 22-30 years) underwent MRI at 3 and 7 T for comparison. Approval for this study was obtained from the Institutional Board of Research Associates of New York University Medical Center and informed consent was obtained from all subjects.

For 2-dimensional imaging, the sequence parameters at 3 T were TR = 5000 ms, TE = 79 ms, FOV = 187 × 250 mm, bandwidth = 399 Hz/pixel, matrix = 192 × 256, resolution = .98 mm × 0.98 mm× 4 mm, numbers of echoes = 25, echo spacing = 6.82 ms, four averages, cceleration factor 2,[17] time of acquisition = 1:27 min. The sequence parameters at 7 T were identical except TE = 82 ms and time of acquisition = 1:47 min.

For 3-dimensional imaging, the sequence parameters were the same at 3 and 7 T: TR = 5000 ms, TE = 94 ms, FOV = 187 × 250 mm, bandwidth = 399 Hz/pixel, matrix = 192 × 256, resolution = .98 mm × .98 mm × 3 mm, number of echoes = 25, 10 slices/slab, slice oversampling 100%, acceleration factor 2, time of acquisition = 8:27 min. Shimming, frequency, and transmitter adjustments were done at the beginning of the study at 3 and 7 T.

SNR were calculated by dividing the mean value of the signal intensity in a small region of interest (ROI) by the standard deviation (SD) of the noise measured in a background ROI of air. Values are given as mean ± SD. The contrast-to-noise ratio (CNR) of two tissues is defined as the difference between their respective SNR, using the notation: $CNR_{Tissue1\text{-}Tissue2} = SNR_{Tissue1} - SNR_{Tissue2}$. It should be noticed, however, that the coils at 3 and 7 T have different numbers of channels, sensitivities, and noise distribution. Hence, the measured SNRs can be used here as guiding parameters for a comparison of the image quality as it can be realized in practice.

Results

Phantoms Experiments

Images obtained at 7 T for the phantom bottles are shown in Figure 3. On TSE images, the oil signal loss was 30% with FatSat and 70% with csFatIR. On 2-dimensional DIR images, while the loss of signal in solution and gel was almost 100%, the oil signal loss was only 20% due to the slight overlap of the DIR pulses on the oil protons. When 2-dimensional DIR + FatSat was performed, the oil signal decreased by 50% due to the additive effect of the FatSat and the DIR pulses. Finally, when 2-dimensional DIR + csFatIR was performed a 95% signal decrease was observed. This preliminary study shows that the csFatIR scheme is much more efficient at 7 T than the standard fat saturation using a gaussian pulse.

Human Experiments

None of the subjects experienced side effects during the MRI protocol at both fields. The inversion times for the volunteers were previously adjusted experimentally. These measured values are very close to the theoretical values calculated with the Redpath method. For WM + CSF suppression at 3 T, TI_1/TI_2 ^{calculated} = 2060/500 ms, TI_1/TI_2 ^{measured} = 2100/470 ms, and at 7 T, TI_1/TI_2 ^{calculated} = 2140/640 ms, TI_1/TI_2 ^{measured} = 2180/550 ms. The theoretical inversion times were calculated from average T_1 relaxation times. These T_1 values must slightly vary from one volunteer to another one, inducing a small difference of a few tens of milliseconds between the theoretical and the experimental inversion times.

Selected 2-dimensional DIR for WM + CSF suppression and 3-dimensional DIR + csFatIR for WM + CSF suppression images obtained at 3 and 7 T from a healthy volunteer are shown in Figures 4 and 5, respectively. The mean SNR measured in regions of interest placed on frontal and occipital WM, frontal and occipital GM, CSF, and bone marrow fat from four healthy volunteer are given in Table 2.

In 2-dimensional images acquired at 3 T, the fat SNR is divided by a factor of 3 with FatSat (but it's inhomogeneous) and 25 with csFatIR (and more homogeneous). At 7 T this factor is approximately 2.5 with FatSat and 22 with csFatIR. csFatIR is more efficient than FatSat at both magnetic fields. It can be noticed on Figure 4 that FatSat is sufficient for a good delineation of GM at 3 T, but not at 7 T where csFatIR is indispensable.

In 2-dimensional, for WM + CSF suppression with DIR + csFatIR : $CNR_{GM\text{-}WM} \approx 18 \pm 3$, $CNR_{GM\text{-}CSF} \approx 10 \pm 4$ at 3 T and $CNR_{GM\text{-}WM} \approx 46 \pm 9$, $CNR_{GM\text{-}CSF} \approx 38 \pm 7$ at 7 T. The SNR of GM at 7 T is the double than at 3 T and the SNR of the suppressed tissues are the same at both fields. Therefore the CNR of GM with CSF and WM increase too at 7 T, but with a lack of signal in the center of the images due to B_1 inhomogeneities (see Fig 4, second row).

In 3-dimensional, for WM + CSF suppression with DIR + csFatIR, $CNR_{GM\text{-}WM} \approx 24 \pm 5$, $CNR_{GM\text{-}CSF} \approx 6 \pm 4$ at 3 T and $CNR_{GM\text{-}WM} \approx 19 \pm 3$, $CNR_{GM\text{-}CSF} \approx 0$ at 7 T. In that case, the SNR and CNR of GM are better at 3 T than at 7 T. It can be noticed here that at 7 T the CSF and GM have almost the same SNR giving no contrast between these two tissues.

This inefficient suppression is mainly due to B_1 inhomogeneities occurring at high field and resulting in very inhomogeneous images as shown in Figure 5B.

Discussion and Conclusion

This preliminary study demonstrates the feasibility of DIR + csFatIR MRI at 7 T. We showed that, especially at 7 T, fat suppression is significantly more efficient with a fat inversion recovery pulse than with the standard fat saturation. It is evident in Figures 4 and 5 that, due to the inherent B_1 inhomogeneities, the desired CNR and SNR are not available throughout the whole of the 7 T images, which exhibit a loss of signal in the center.

In 2-dimensional, the SNR of GM is twice better at 7 T than at 3 T, thus providing a better contrast between GM and the suppressed tissues at 7 T. This SNR increase reflects a linear increase of signal with magnetic field strength. It should be kept in mind, however, that the coils used in the present study have different sensitivity and noise distribution and, as a consequence, our experiments do not allow an absolute quantification of the real field-dependent increase of SNR.

Unlike 2-dimensional images, the 3-dimensional images acquired at 3 T show better SNR and CNR for GM than the ones acquired at 7 T. The loss of SNR at 7 T is mainly due to B_1 inhomogeneities during the transmission and the reception components of the sequence. B_1 inhomogeneities have a higher impact in 3-dimensional than in 2-dimensional imaging. At 7 T, increasingly non-perfect 180° pulses during the TSE sequence lead to loss of signal for the non-suppressed tissues and reappearance of signal from the suppressed tissues, with a consequent loss of SNR and CNR. For reception, due to the loss of central sensitivity of the 24-channel array coil at 7 T, the signal in the middle of the brain is lower than the signal from the edges of the brain.

It has previously been reported that the contrast in multislice MR images obtained using fast spin echo readout is affected by the magnetization transfer (MT) effects.[18] This MT effect is more relevant on signal intensity from tissue types with a large bound water component such as white matter. This does not apply to our experiments since we used non-selective inversion pulses and, therefore, the DIR images were obtained for only one slice in 2-dimensional and one slab in 3-dimensional.

In conclusion, DIR is feasible at 7 T, despite the problems associated with B_1 in-homogeneity. While the 2-dimensional images exhibit an increase of SNR and CNR at 7 T, the 3-dimensional images show a lower quality in terms of SNR and CNR than the corresponding ones obtained at 3 T. The field in-homogeneity at 7 T, by affecting the DIR signal suppression, can especially hamper the use of the method for GM segmentation and the accuracy of volumetric measures. Further experimental and theoretical investigation will focus on the improvement of the homogeneity of the DIR images at 7 T by using pulse adjustments, B_1 shimming and sensitivity adjustment of individual coil channels. This should enhance the performance of 3-dimensional DIR imaging at 7 T enabling us to take advantage of higher SNR to increase the spatial resolution in a reasonable acquisition time.

The sequence is suitable for application to many disease processes involving GM.[7–9] In MS, DIR has been shown to reliably improve intra-cortical lesions and its future application at higher magnetic field has the potential to help elucidate cognitive impairment, which is a quite common but yet poorly understood symptom in patients with MS. In MRI-negative patients with refractory epilepsy, DIR has been reported to identify "occult" focal abnormalities and its future application might contribute to pre-surgical evaluation. Furthermore, in degenerative disorders such as Alzheimer's disease, where it is important to reliably assess volume or thickness of the hippocampus and the entorhinal cortex, DIR might prove of use. The sequence allows for the acquisition of images of the GM with minimum partial volume contamination which, in turn, is advantageous for brain segmentation techniques.

Acknowledgments

This study was supported in part by NIH RO1 NS051623.

References

1. Bydder GM, Young IR. MR imaging: clinical use of the inversion recovery sequence. J Comput Assist Tomogr 1985;9(4):659–675. [PubMed: 2991345]
2. Redpath TW, Smith FW. Technical note: use of a double inversion recovery pulse sequence to image selectively grey or white brain matter. Br J Radiol 1994;67(804):1258–1263. [PubMed: 7874427]
3. Pouwels PJ, Kuijer JP, Mugler JP 3rd, et al. Human gray matter: feasibility of single-slab 3D double inversion-recovery high-spatial-resolution MR imaging. Radiology 2006;241(3):873–879. [PubMed: 17053197]
4. Boulby PA, Symms MR, Barker GJ. Optimized interleaved whole-brain 3D double inversion recovery (DIR) sequence for imaging the neocortex. Magn Reson Med 2004;51(6):1181–1186. [PubMed: 15170838]
5. Wattjes MP, Lutterbey GG, Gieseke J, et al. Double inversion recovery brain imaging at 3T: diagnostic value in the detection of multiple sclerosis lesions. AJNR Am J Neuroradiol 2007;28(1):54–59. [PubMed: 17213424]
6. Geurts JJ, Pouwels PJ, Uitdehaag BM, et al. Intracortical lesions in multiple sclerosis: improved detection with 3D double inversion-recovery MR imaging. Radiology 2005;236(1):254–260. [PubMed: 15987979]
7. Frisoni GB, Testa C, Zorzan A, et al. Detection of grey matter loss in mild Alzheimer's disease with voxel based morphometry. J Neurol Neurosurg Psychiatry 2002;73:657–664. [PubMed: 12438466]
8. Rugg-Gunn FJ, Boulby PA, Symms MR, et al. Imaging the neocortex in epilepsy with double inversion recovery imaging. Neuroimage 2006;31(1):39–50. [PubMed: 16460962]
9. Catalaa I, Fulton JC, Zhang X, et al. MR imaging quantitation of gray matter involvement in multiple sclerosis and its correlation with disability measures and neurocognitive testing. AJNR Am J Neuroradiol 1999;20(9):1613–1618. [PubMed: 10543630]
10. Nakada T Clinical application of high and ultra high-field MRI. Brain Dev 2007;29(6):325–335. [PubMed: 17113259]
11. Hu X, Norris DG. Advances in high-field magnetic resonance imaging. Annu Rev Biomed Eng 2004;6:157–184. [PubMed: 15255766]
12. Vaughan JT, Garwood M, Collins CM, et al. 7T vs. 4T: RF power, homogeneity, and signal-to-noise comparison in head images. Magn Reson Med 2001;46(1):24–30. [PubMed: 11443707]
13. Meara SJ, Barker GJ. Evolution of the longitudinal magnetization for pulse sequences using a fast spin-echo readout: application to fluid-attenuated inversion-recovery and double inversion-recovery sequences. Magn Reson Med 2005;54(1):241–245. [PubMed: 15968670]

14. Wansapura JP, Holland SK, Dunn RS, et al. NMR relaxation times in the human brain at 3.0 Tesla. J Magn Reson Imaging 1999;9(4):531–538. [PubMed: 10232510]
15. Bottomley PA, Foster TH, Argersinger RE, et al. A review of normal tissue hydrogen NMR relaxation times and relaxation mechanisms from 1–100 MHz: dependence on tissue type, NMR frequency, temperature, species, excision, and age. Med Phys 1984;11(4):425–448. [PubMed: 6482839]
16. Rooney WD, Johnson G, Li X, et al. Magnetic field and tissue dependencies of human brain longitudinal $^{1}H_2O$ relaxation in vivo. Magn Reson Med 2007;57:308–318. [PubMed: 17260370]
17. Griswold MA, Jakob PM, Heidemann RM, et al. Generalized autocalibrating partially parallel acquisitions (GRAPPA). Magn Reson Med 2002;47(6):1202–1210. [PubMed: 12111967]
18. Meara SJ, Barker GJ. Impact of incidental magnetization transfer effects on inversion-recovery sequences that use a fast spin-echo readout. Magn Reson Med 2007;58(4):825–829. [PubMed: 17899590]

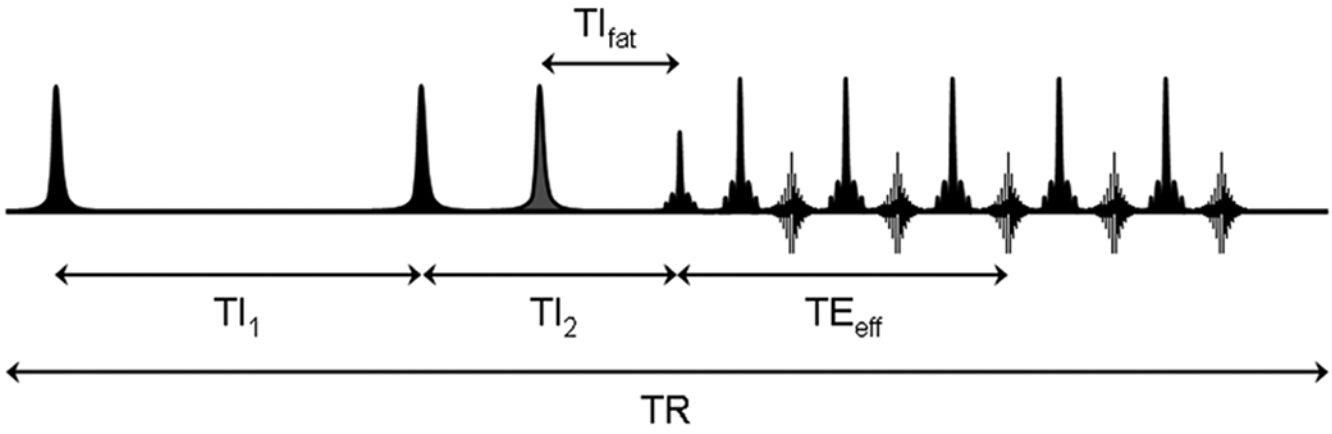

Fig 1.

Pulse chronogram of the Turbo Spin Echo Double Inversion Recovery with chemical shift Fat Inversion (TSE DIR + csFatIR). Hyperbolic secant adiabatic pulses are used for both DIR and csFatIR. TI_1 and TI_2 are the first and second inversion times for DIR. TI_{fat} is the inversion time for fat after the inversion pulse at fat frequency (in grey). In this example, the turbo factor is 5.

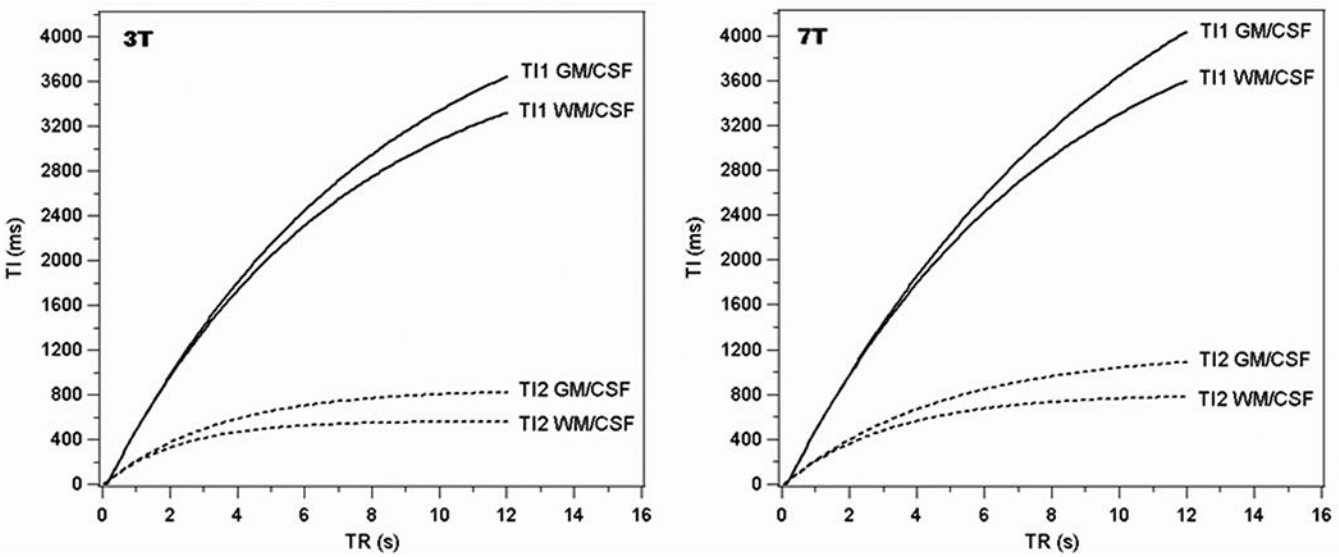

Fig 2.

Fitting curves for TI_1 and TI_2 as functions of TR (ms), for WM + CSF and GM + CSF suppression obtained at 3 and 7 T. The fitting parameters are given in Table 1.

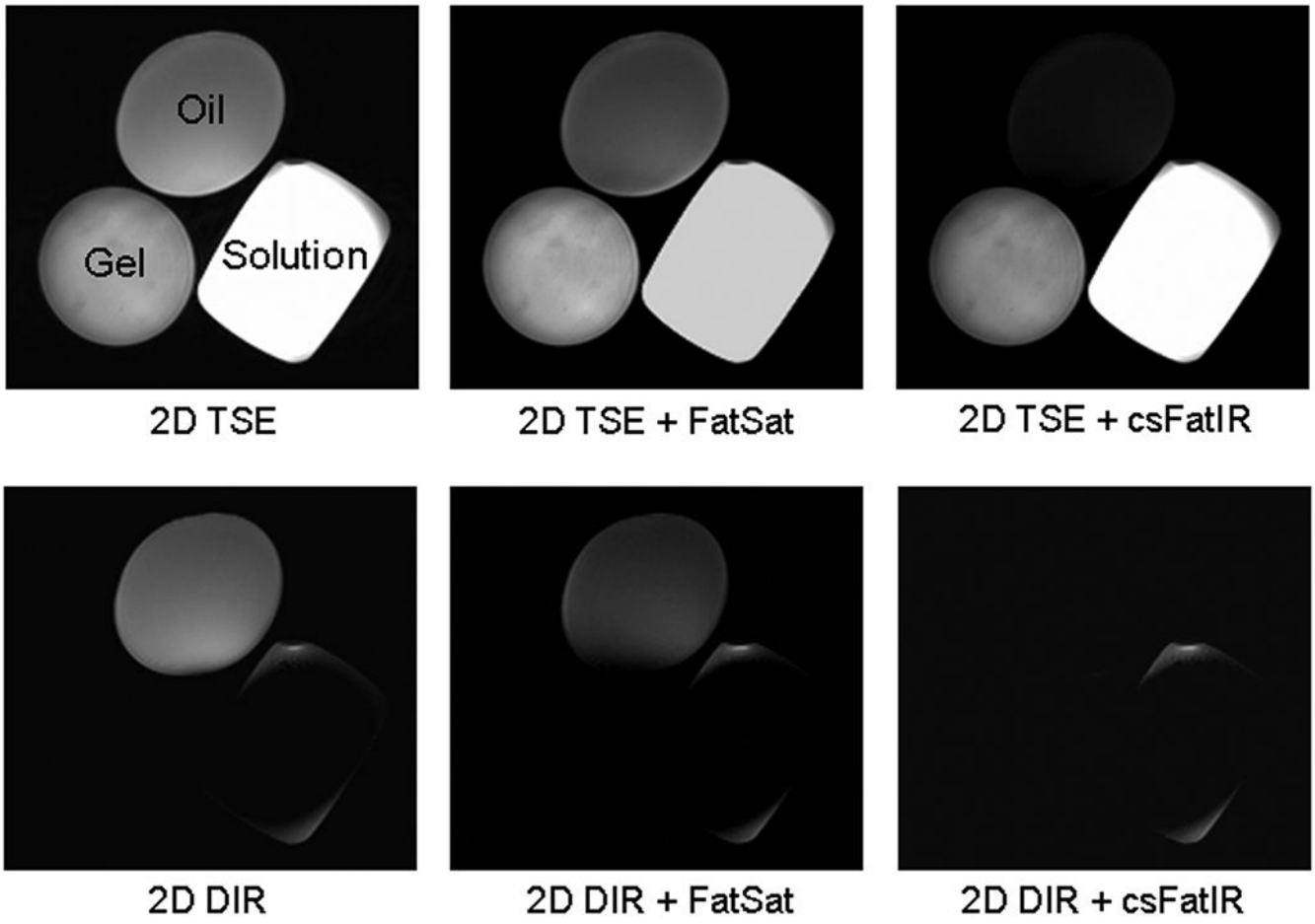

Fig 3.

2-Dimensional TSE and 2-dimensional DIR images obtained from phantoms at 7 T DIR images with standard fat saturation (FatSat) are compared with DIR images with chemical shift Fat Inversion recovery (csFatIR). Three phantoms were used: one bottle of vegetable oil, T_1 = 330 ms, one bottle of gel Agar 4% + NaCl 15 mM, T_1 = 2470 ms, and one bottle of solution of $6H_2O$ + 1.78 g/L of $CuSO_4$ + 1.61 g/L of NaCl, T_1 = 190 ms. For the suppression of the gel and solution signals by DIR, for TR = 5000 ms, the inversion times were TI_1 = 1500 ms and TI_2 = 130 ms. For csFatIR, TI_{fat} = 230 ms. Note the better fat signal suppression with DIR + csFatIR than with DIR + FatSat.

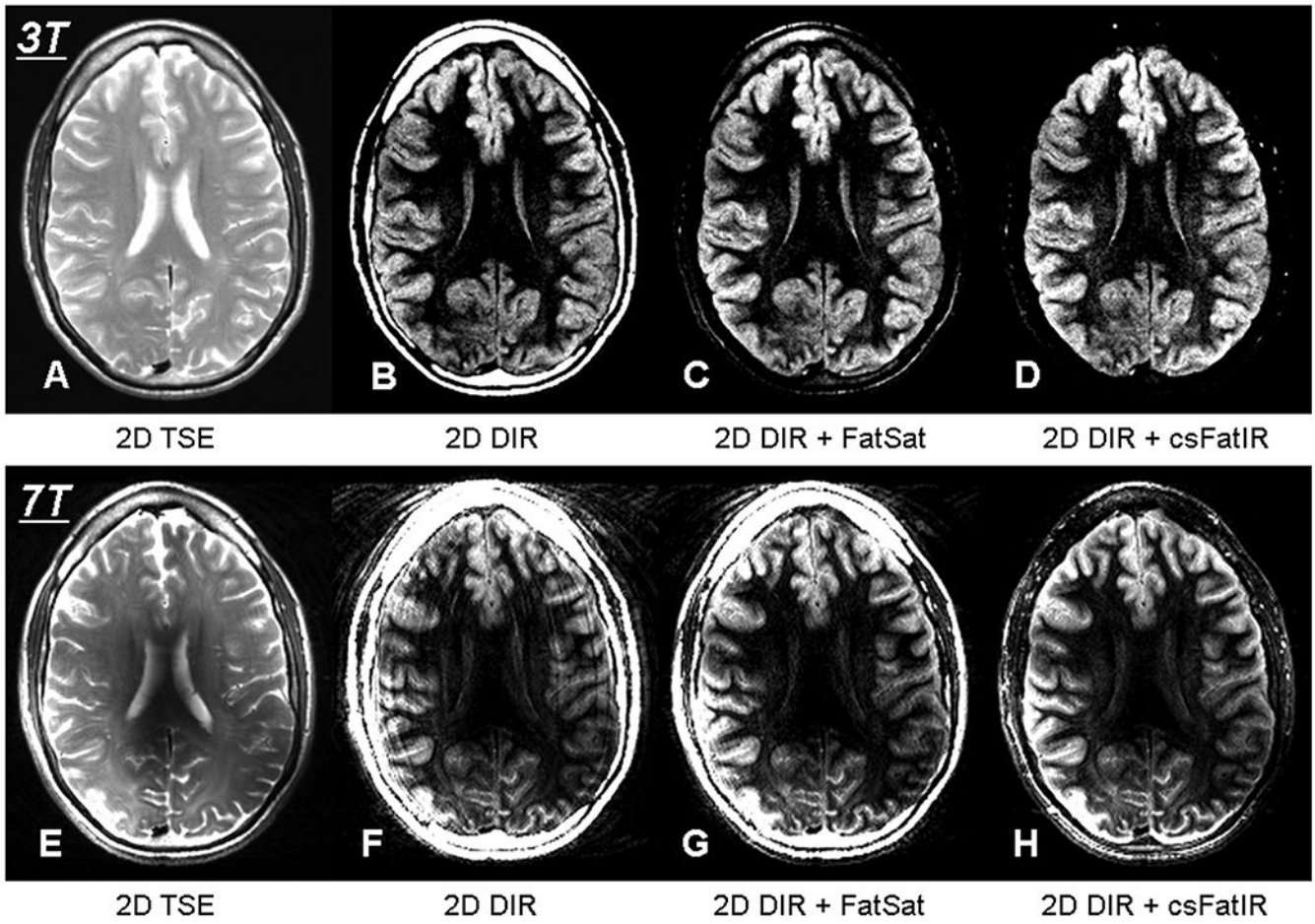

Fig 4.

2-Dimensional brain images acquired on a volunteer at 3 T (first row) and 7 T (second row), without tissue suppression (A, E) and with WM + CSF suppression: 2-dimensional DIR (B, F), 2-dimensional DIR + FatSat (C, G), 2-dimensional DIR + csFatIR (D, H). Note the more efficient fat suppression with csFatIR (D, H) than with FatSat (C, G).

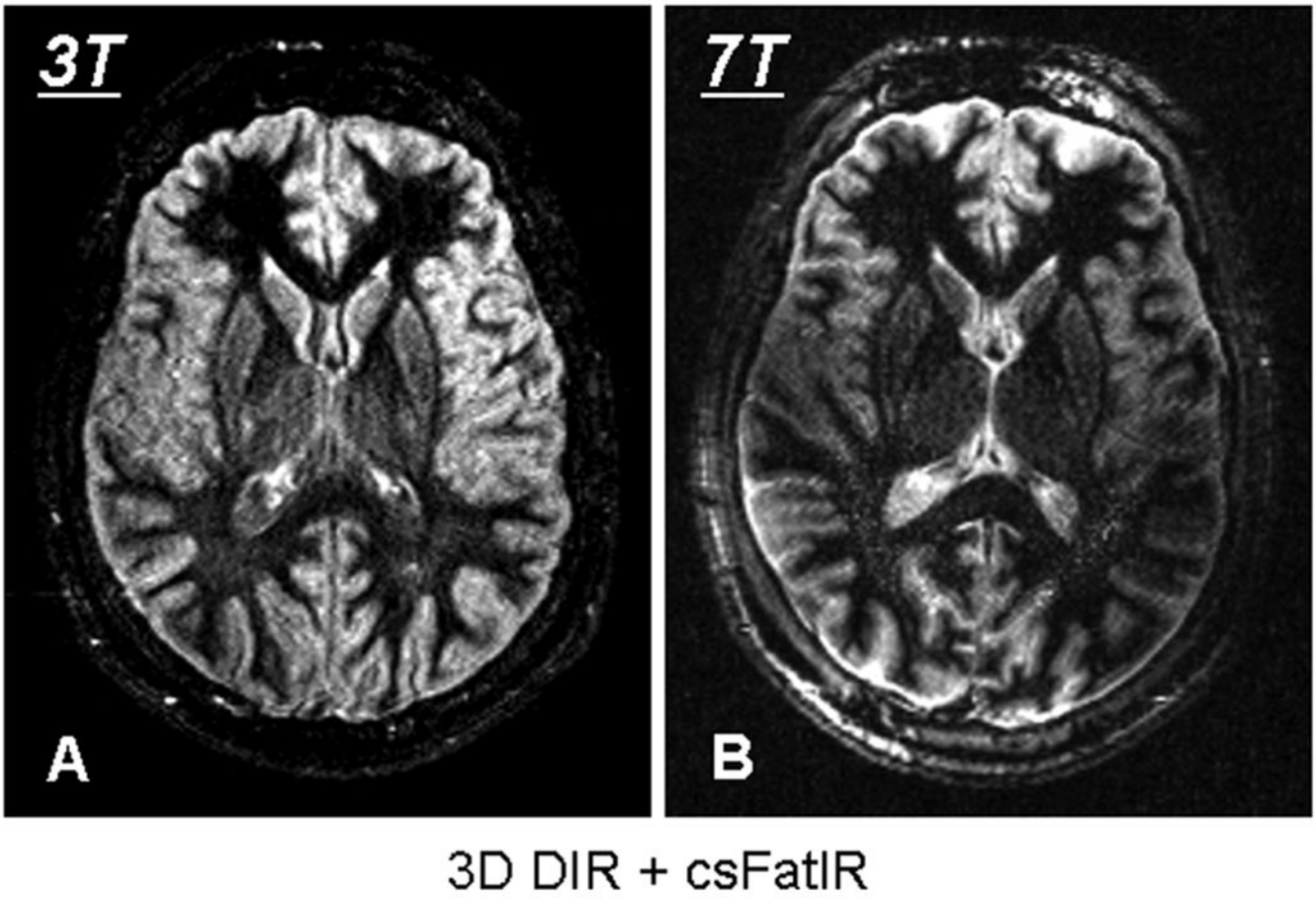

Fig 5.
3-Dimensional brain images acquired on a volunteer with WM + CSF suppression: 3-dimensional DIR + csFatIR at 3 T (A) and 7 T (B).

Table 1.

Fitting Parameters for the Theoretical TI_1 and TI_2 as Functions of TR (ms) for DIR WM + CSF and GM + CSF Acquired at 3 and 7 T

Magnetic field	Suppressed tissues	TI (ms)	A* (ms)	B* (ms)	C* (ms^{-1})
3 T	WM + CSF	TI_1	4063	−4135	-1.435×10^{-4}
		TI_2	564	−571	-4.426×10^{-4}
	GM + CSF	TI_1	4722	−4807	-1.249×10^{-4}
		TI_2	847	−859	-2.988×10^{-4}
7 T	WM + CSF	TI_1	4619	−4701	-1.272×10^{-4}
		TI_2	800	−811	-3.105×10^{-4}
	GM + CSF	TI_1	5825	−5913	$-.996 \times 10^{-4}$
		TI_2	1183	−1197	-2.117×10^{-4}

*A, B, C: Fitting parameters of the function $TI(TR) = A + B \cdot e^{C \cdot TR}$.

Table 2.

SNR Values (Mean Value ± Standard Deviation) Measured from Several Brain Tissues on 2-Dimensional and 3-Dimensional DIR Images (for WM + CSF Suppression) Acquired at 3 and 7T from Four Healthy Volunteer

Magnetic field	Tissues	2-Dimensional DIR	2-Dimensional DIR + FatSat	2-Dimensional DIR + csFatIR	3-Dimensional DIR + csFatIR
3 T	CSF	23 ± 3	23 ± 3	21 ± 2	27 ± 4
	Frontal WM	10 ± 3	10 ± 3	12 ± 3	9 ± 3
	Occipital WM	12 ± 3	12 ± 3	15 ± 3	10 ± 3
	Mean WM	11 ± 3	11 ± 3	13.5 ± 3	9.5 ± 3
	Frontal GM	35 ± 3	34 ± 3	33 ± 3	35 ± 3
	Occipital GM	33 ± 3	31 ± 3	30 ± 3	31 ± 3
	Mean GM	34 ± 3	32.5 ± 3	31.5 ± 3	33 ± 3
	Bone marrow fat	100 ± 28	34 ± 8	4 ± 2	19 ± 5
7 T	CSF	27 ± 4	17 ± 4	25 ± 4	25 ± 2
	Frontal WM	18 ± 8	12 ± 3	15 ± 6	6 ± 2
	Occipital WM	18 ± 4	14 ± 3	18 ± 3	6 ± 2
	Mean WM	18 ± 6	13 ± 3	16.5 ± 5	6 ± 2
	Frontal GM	62 ± 7	49 ± 6	66 ± 9	29 ± 3
	Occipital GM	60 ± 8	45 ± 6	60 ± 8	21 ± 2
	Mean GM	61 ± 8	47 ± 6	63 ± 9	25 ± 3
	Bone marrow fat	689 ± 167	269 ± 70	31 ± 12	27 ± 3